Mansoura Journal of Chemistry Vol. 35 (2), December, 2008.

EVALUATION OF ARYLAZO INDOLE DERIVATIVES AS CORROSION INHIBITORS FOR *A*-BRASS IN HNO_3 SOLUTION

A. S. Fouda* and Huda Mahfouz
Department of Chemistry, Faculty of Science, Mansoura University, Mansoura-35516, EGYPT – Tel. +20 (2) 50 2245730; Fax +20 (2) 502246781; *Corresponding author: email:asfouda@yahoo.com

(Recevied: 1 / 7 / 2008)

ABSTRACT

The influence of some arylazo indole derivatives on the corrosion rate of α-brass (Cu/Zn: 70/30) in 2M HNO_3 has been studied. The inhibition efficiency obtained by weight loss and galvanostatic polarization techniques was found to be in good agreement and reveal that arylazo indole derivatives are very efficient inhibitors. The inhibition efficiency increases with an increase in inhibitor concentration, but decreases with an increase in temperature. The adsorption of these compounds on the α-brass surface follows a Frumkin's adsorption isotherm. The electrochemical results indicated that all the investigated compounds act as mixed-type inhibitors. Thermodynamic functions for both dissolution and adsorption processes were determined and discussed.

Keywords: corrosion inhibition; α-brass; synergistic effect; HNO_3; arylazo indole derivatives.

1. INTRODUCTION

Brass is composed of copper and zinc alloy (ordinary brass), corrosion and corrosion inhibition of brass alloys, in general, and α-brass, in particular, have received a great attention in different media like a material commonly used in the manufacture of electrodes for batteries, decorative or functional objects and parts of engines and machinery, as well as pipelines and tubes, and it is easily cut and polished. Electro-analytical techniques are powerful tools to study brass since they offer

valuable information about the phase and chemical composition. [**Stevanovic et al., (1992)**]. A number of studies have recently appeared in the literature, [**Rehan et al., (2003); Haquea & Faris (2008) and Mihit et al., (2006)**]. On the topic of the corrosion inhibition of α-brass in acidic medium. But little work appears to have been done on the inhibition of α-brass alloys in nitric acid using arylazo indole derivatives.

The present work was designed to study: i) corrosion inhibition of α-brass in nitric acid solution by some arylazo indole derivatives using weight-loss and galvanostatic polarization techniques; ii) the effect of substituted groups on the inhibition efficiency and iii) the effect of temperature on the corrosion rate in order to calculate some thermodynamic parameters related to the corrosion process.

2. EXPERIMENTAL TECHNIQUE

2.1. Materials

The experiments were performed with α-brass having the chemical compositions (Cu/Zn: 70/30). The inhibitors used in this study were selected from arylazo indole derivatives and are listed below:

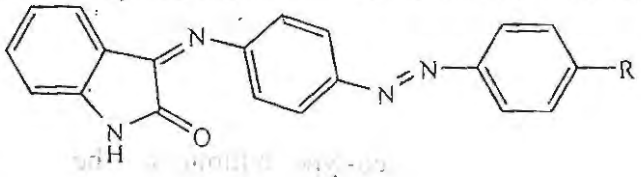

Where: R= OCH_3 **(a)**
= CH_3 **(b)**
= H **(c)**
= NO_2 **(d)**

2.1.1. Preparation of inhibitors (arylazo indole derivatives)

Arylazo indole derivatives **(a-d)** were prepared by adding a mixture of isatin (0.01 mol), *p*-aminoazobenzene derivatives (0.01 mol) and then heated in an oil bath at 170°C for 2h in the presence of freshly fused sodium acetate. After cooling, the solid product was washed with water, dried and recrystallized from ethanol to give 3-arylazoindol-2-one **(a-d)** derivatives. Formations of these compounds were checked by both elemental and spectral analyses. In general, the IR spectra gave an absorption bands at 1730, 1658 and 1614 cm^{-1} due to the CON, C=N and N=N functions, respectively. Moreover, the mass spectrum of

compounds (**b, c, d**) showed the molecular ion peaks at 427 (M^+, 25%), 371 (M^+, 100%) and 356 (M^+, 100%), respectively. Finally, the ^{1}H-NMR of compound (**a**) reveals bands at δ 4.1 (s, 3H, OCH_3), 7.2-8.3 (m, 12H, Ar-H), 9.9 (s, 1H, NH).

100 ml stock solutions (10^{-3} mol l^{-1}) of compounds **(a-d)** were prepared by dissolving an accurately weighed quantity of each material in an appropriate volume of absolute ethanol, then the required concentrations (1×10^{-6} - 11×10^{-6} mol l^{-1}) were prepared by dilution with bidistilled water.

Nitric acid solution was prepared by diluting the appropriate volume of the concentrated chemically pure acid (BDH grade), with bidistilled water and its concentration was checked by standardarized solution of NaOH.

100 ml stock solution (10^{-2} mol l^{-1}) of KSCN (BDH grade) is prepared by dissolving an accurately weighed quantity of this material in an appropriate volume of bidistilled water.

Two different techniques have been employed for studying the corrosion inhibition of α-brass by arylazo indole derivatives, these are: i) chemical technique (weight loss method) and ii) electrochemical technique (galvanostatic polarization method).

2.2. Chemical technique (weight-loss method):

The reaction basin used in this method was graduated glass vessel 6 cm inner diameter and having a total volume of 250 ml. 100 ml of the test solution were employed in each experiment. The test pieces were of dimensions 2 x 2 x 0.2 cm. They were mechanically polished with emery paper (a coarse paper was used initially and then progressively finer grades were employed), ultrasonically degreased in methanol, rinsed in doubly distilled water and finally dried between two filter papers and weighed. The test pieces were suspended by suitable glass hooks at the edge of the basin, and under the surface of the test solution by about 1cm. After specified periods of time, 3 test pieces were withdrawn from the test solution, rinsed in doubly distilled water, dried as before and weighed again. The average weight loss at a certain time for each set of three samples was taken.

2.3. Electrochemical technique (galvanostatic polarization method):

Three different types of electrodes were used during polarization measurements, the working electrode was α-brass electrode, which cut

from the α-brass sheets, of thickness 0.2 cm. The electrode was of dimensions 1cm x 1cm and was weld from one side to a copper wire used for electric connection. The samples were embedded in glass tube using epoxy resin. **[Otieno-Alego et al., (1992)]** The electrode was prepared before immersion in the test solution as in the case of weight loss. Saturated calomel electrode and a platinum coil were used as reference and auxiliary electrodes, respectively. A constant quantity of the test solution (100 ml) was taken in the polarization cell. A time interval of about 30 min was given for the system to attain steady state. Both cathodic and anodic polarization curves were recorded galvanostatically using Amel galvanostat (Model 549) and digital multimeters (Fluke-73) were used for accurate measurements of the potentials and current density. All the experiments were carried out at 30 ±1°C by using an ultra circulating thermostat.

3. RESULTS AND DISCUSSION

3.1. Weight-loss measurements

Figure (1) shows the weight loss-time curves for the brass in different concentrations of nitric acid (0.1 – 3.0 mol l^{-1}). The plots of this figure indicate that the weight loss increases with the increase immersion time. In addition, at a given immersion time the weight loss increases with increasing nitric acid concentration (especially at high concentrations). Figure (2) shows the weight loss-time curves for the brass in 2 mol l^{-1} HNO_3 in absence and in presence of different concentration of compound **(a)**. Similar curves are obtained in the presence of other organic compounds **(b, c, d)**, but not shown. From the plots of Figure (2) and similar one the weight loss, and corrosion rate (Rw) were calculated. From the values of (Rw) in absence and in presence of different concentrations of additives, the inhibition efficiency (I %) was calculated for the additives **(a-d)** and listed in Table (1). The results of Table (1) show that the inhibition efficiency of all additives increases with the increase of their concentrations in the corrosive medium. It is thus obvious that increase of bulk concentration and consequently, increase of surface area coverage by the additive retards the dissolution of α-brass. The order of the inhibition efficiency of the additive compounds in 2 mol l^{-1} nitric acid solution over most of the concentration ranges used after 120 minutes are: **a > b > c > d**.

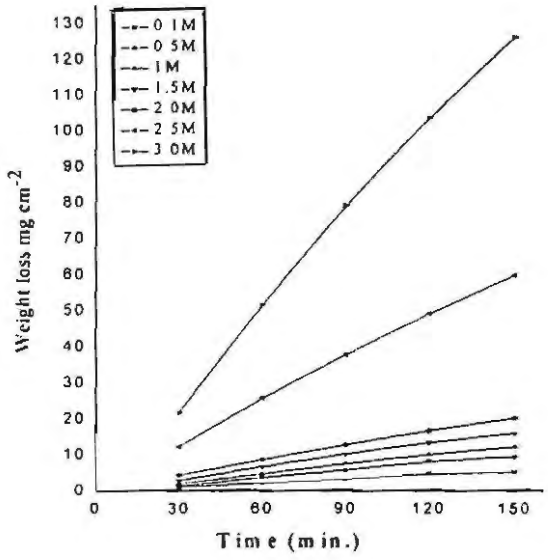

Fig. (1): weight loss-time curves in different concentrations of HNO_3 at 30°C.

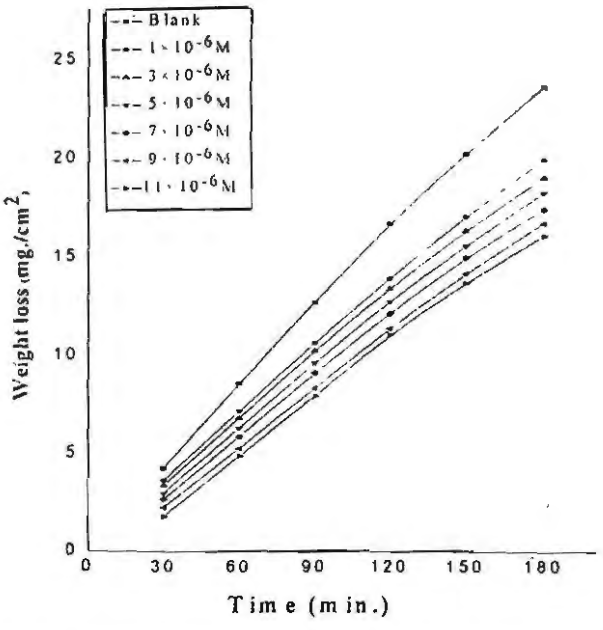

Fig. (2): Weight loss-time curves for α-brass in 2M HNO_3 in presence and absence of different concentrations of compound (a) at 30°C.

Table (1): Variation of the inhibition efficiency, (%) of the Studied compounds with their molar concentrations after 120 min.; immersion at 30°C.

Concentration (M)	Inhibition efficiency, %			
	a	**b**	**c**	**d**
$1x10^{-6}$	16.7	13.5	11.4	7.2
$3x10^{-6}$	19.8	17.2	15.7	12.3
$5x10^{-6}$	23.7	20.6	18.2	14.5
$7x10^{-6}$	27.4	23.3	21.6	17.9
$9x10^{-6}$	32.0	28.5	26.8	22.8
$11x10^{-6}$	33.9	31.6	28.7	26.6

3.2. Adsorption isotherms:

The degree of surface coverage (θ) which represents the part of metal surface covered by inhibitor molecules was calculated from (I %) using the following equation:

$$\theta = \frac{I\%}{100} \quad (1)$$

The calculated values of (θ) are listed in Table (2). The degree of surface coverage was found to increase with increasing the concentration of the used additives. Attempts were made to fit θ values to various isotherms including Frumkin, Freundlich, Langmuir and Temkin. By far, the best fit was obtained with Frumkin's isotherm which has the following equation:

$$\theta = Const + (2.303/f) \log C \quad (2).$$

$$\text{Where, } f = 1/RT\,[d(\Delta G_a^{\circ} / d\theta] \quad (3),$$

Where, C= inhibitor concentration and ΔG_a°= the free energy of adsorption. Figure (3) represents the relation between θ and log C for the inhibitors **(a-d)**. The plots of Fig (3) have S-shape which means that the Frumkin's adsorption isotherm is obeyed. From these results it could be concluded that there is a kind of interaction between the molecules adsorbed at the metal surface.

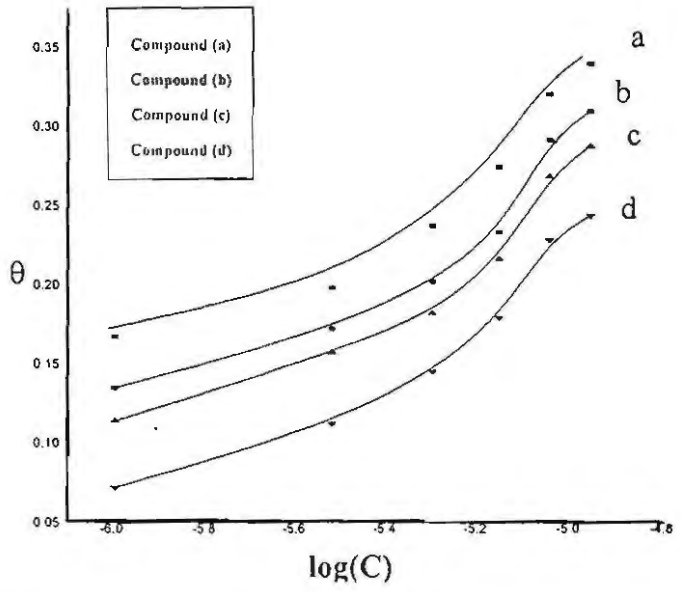

Fig. (3): Log(C) - Θ curves for the different compounds

Table (2): Variation of degree of surface coverage (θ) of different compounds **(a-d)** with their molar concentrations at 30°C from weight loss measurements at 120 min., immersion.

Concentration (M)	Surface coverage (θ)			
	a	**b**	**c**	**d**
$1x10^{-6}$	0.167	0.135	0.114	0.072
$3x10^{-6}$	0.189	0.172	0.157	0.123
$5x10^{-6}$	0.237	0.206	0.182	0.145
$7x10^{-6}$	0.274	0.233	0.216	0.179
$9x10^{-6}$	0.320	0.285	0.268	0.228
$11x10^{-6}$	0.339	0.319	o.287	0.266

3.3. Effect of temperature on the corrosion inhibition of α-brass:

The dissolution of α-brass in 2 mol l^{-1} nitric acid increases by increasing temperatures as shown in Figure (4). The dissolution of α-brass in 2 mol l^{-1} nitric acid in presence of different inhibitors at $11x10^{-6}$ mol l^{-1} was studied by weight loss method over a temperature range 30-50°C. Figure (5) show the weight loss-time curves for the brass in 2 mol l^{-1} HNO_3 containing (5×10^{-6} mol l^{-1}) of compound (**a**) at different temperatures (30–50°C). Similar weight loss-time curves are obtained for the other compounds (**b, c, d**), but not shown. The weight loss-time curves obtained in presence of additives indicate that the rate of α-brass dissolution increases as the temperature increase, but at lower rate than in uninhibited solutions. The inhibition efficiency of the additives decreases with rise in temperature which proves that the adsorption of these compounds on the surface of α-brass occurs through physical adsorption of the additives on the metal surface. Desorption is aided by increasing the reaction temperature. The apparent activation energy (E_a^*), the enthalpy of activation (ΔH^*) and the entropy of activation (ΔS^*) for the corrosion of α-brass in 2 mol l^{-1} nitric acid solution in the absence and presence of different concentrations of arylazo indole compounds were calculated from Arrhenius-type equation:

$$\text{Rate} = A \exp(-E_a^*/RT) \quad (4)$$

Also, the transition-state equation:

$$\text{Rate} = RT/Nh \exp(\Delta S^*/R) \exp(-\Delta H^*/RT) \quad (5)$$

Where (A) is the frequency factor, (h) is the Planck's constant, (N) is Avogadro's number and (R) is the universal gas constant. A plot of log Rate vs. (1/T) and log (Rate/T) vs. (1/T) Figures (6) and (7) give straight lines with slope of ($-E_a^*/2.303R$), and ($-\Delta H^*/2.303R$), respectively. The intercepts will be (A) and (log $R/Nh+\Delta S^*/2.303R$) for Arrhenius and transition state equations, respectively. The calculated values of the apparent activation energy, (E_a^*), activation entropies, (ΔS^*), and activation enthalpies, (ΔH^*), are given in Table (3). The almost similar values of (E_a^*) suggested that the inhibitors are similar in the mechanism of action and the order of efficiency may be related to the preexponential factor (A) in equation (4). This is further related to concentration, steric effects and metal surface characters. Generally, one can say that the nature and concentration of electrolyte affect greatly the activation energy for the corrosion process. The order of the inhibition efficiencies of arylazo indole derivatives as gathered from the increase in

(E_a^*) and (ΔH^*) values and decrease in (ΔS^*) values are as follow: **a > b > c > d**.

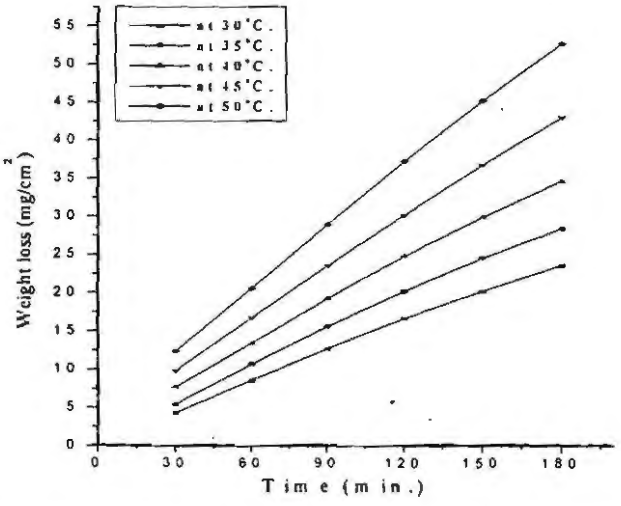

Fig. (4): Weight loss-Time curves for α-brass in 2 mol l^{-1} HNO_3 at different temperatures.

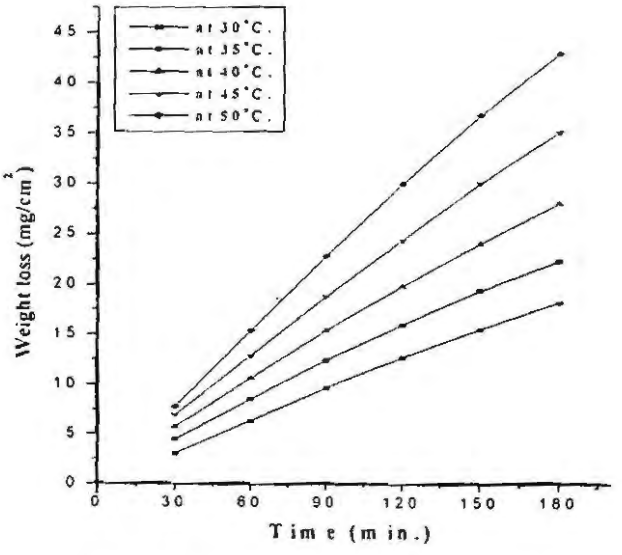

Fig.(5): Weight loss-Time curves for α-brass in 2 mol l^{-1} HNO_3 in presence of ($5x10^{-6}$ mol l^{-1}) of compound (a) at different temperatures.

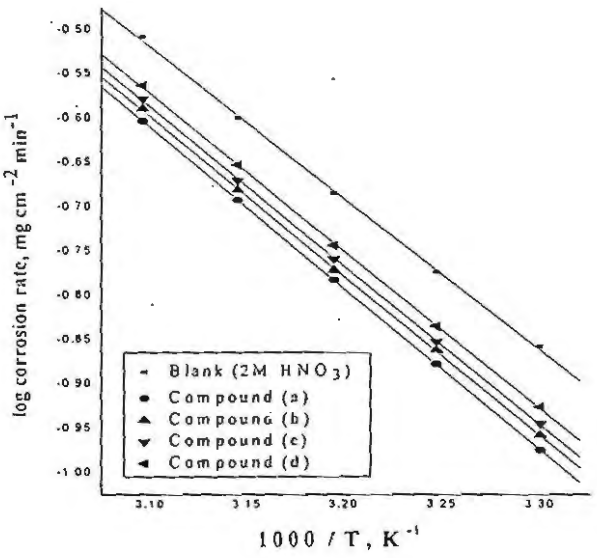

Fig (6): Arrhenius plot for the corrosion of the α-brass in 2 M HNO_3 in presence and absence of different compounds

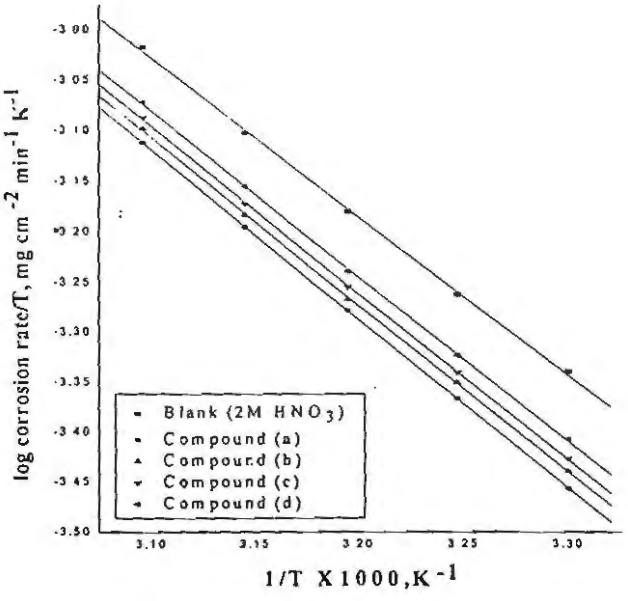

Fig. (7): log K/T Vs 1/T for the corrosion rate of the α-brass in 2 M HNO_3 in presence and absence of different compounds

Table (3): Activation energy (E_a^*), enthalpy change (ΔH_a^*) and entropy change (ΔS_a^*) for the α-brass in 2 mol l^{-1} nitric acid in absence and presence of different inhibitors.

Compound	$-E_a^*$(k J mol^{-1})	ΔH_a^*(k J mol^{-1})	$-\Delta S_a^*$(J mol^{-1} K^{-1})
Blank	32.739	30.18	161.88
a	34,020	31.46	158.92
b	34.210	31.65	158.45
c	34.322	31.76	158.27
d	34.816	32.26	157.18

3.4. Synergistic effect:

Some anions are found to enhance the inhibitive effect of several nitrogen containing organic compounds in acid solutions. **[Hackerman et al., (1966); Murakawa et al., (1968); Rawat & Udayabhanu (1987) and Chatterjee et al., (1991)]** In the present paper the influence of thiocyanide ions on the inhibitive performance of arylazo indole compounds has been studied using weight loss technique. Figure (8) represents the weight loss-time curves for α-brass dissolution in 2 mol l^{-1} nitric acid for various concentrations of compound (**a**) and at specific concentration (1X 10^{-2} mol l^{-1}) of this salt. Similar weight loss-time curves are obtained for the other compounds (**b, c, d**), but not shown. The values of inhibition efficiency (%In.) for various concentrations of inhibitors in the presence of (1X 10^{-2} mol l^{-1}) of KSCN are given in Table (4). The synergistic inhibition effect was evaluated using a parameter, S_θ, obtained from the surface coverage values (θ) of the anion, cation and **[Aramaki et al., (1969)]** calculated the synergism parameter S_θ using the following equation:

$$S_\theta = 1-\theta_{1+2}/1-\theta'_{1+2} \quad (5)$$

where: $\theta_{1+2} = (\theta_1+\theta_2)-(\theta_1\theta_2)$;

θ_1= surface coverage by anion;

θ_2= surface coverage by cation;

θ'_{1+2}= measured surface coverage by both the anion and cation.

The corresponding values of S_θ are shown in Table (5). As can be seen from this Table, values nearly equal to unity were obtained, which suggests that the enhanced inhibition efficiencies caused by the addition of thiocyanide to arylazo indole compounds is due mainly to the synergistic effect.

Finally, It is observed that (%In.) of the inhibitors increases in the presence of (SCN^-) ions due to synergistic effects **[Cahskan & Bilgic (2000)]**. Adsorption of arylazo indole compounds at the α-brass/solution interface occurs through physical adsorption *via* electron rich centers, *i.e.* benzene ring through its π-electrons and nitrogen atom through their lone pairs of electrons by donation of electrons to the empty d-orbital of the metal **[Hang et al., (1988)]**. It is known that (SCN^-) anions have strong interactions with α-brass surfaces owing to chemisorption **[Ammar, et al., (1968)] and Jestonek & Szklarska (1983)]**. The strong chemisorption of (SCN^-) anions on the metal surface is responsible for the synergistic effect of thiocyanide anions in combination with cation of the inhibitor. The cation is then adsorbed by coulombic attraction on the metal surface where (SCN^-) anions are already adsorbed by chemisorption. Stabilization of adsorbed (SCN^-) anions with cations leads to greater surface coverage and therefore greater inhibition..

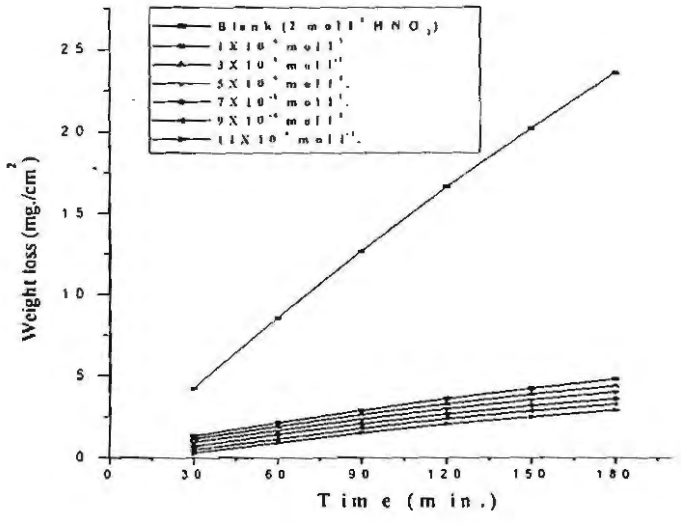

Fig. (8): Weight loss-Time curves for α-brass in 2 mol l^{-1} HNO_3 in presence and absence of different concentrations of compound (a) and in presence of ($1x10^{-2}$ mol l^{-1}) of KSCN at 30°C.

Table (4): Values of inhibition efficiencies (%In.) of different arylazo indole compounds in the presence of ($1X10^{-2}$ mol l^{-1}) KSCN for the corrosion of α-brass in 2 mol l^{-1} HNO_3 at 30°C. Duration of the experiment: 120 min., immersion.

Concentration (M)	Inhibition efficiency (%In)			
	a	**b**	**c**	**d**
$1x10^{-6}$	77.72	76.73	75.89	74.08
$3x10^{-6}$	80.09	87.44	77.29	75.65
$5x10^{-6}$	82.35	80.42	79.17	77.08
$7x10^{-6}$	84.39	82.86	80.87	78.37
$9x10^{-6}$	86.34	85.16	82.7	80.04
$11x10^{-6}$	88.29	86.73	84.32	81.75

Table (5): Synergism parameter (S_0) for various concentrations of different arylazo indole compounds in the presence of ($1X10^{-2}$ mol l^{-1}) KSCN. Duration of the experiment: 120 min., immersion.

Concentration (M)	Synergism parameter (S_θ)			
	a	**b**	**c**	**d**
$1x10^{-6}$	0.832	1.031	1.008	0.986
$3x10^{-6}$	1.117	1.046	1.009	0.973
$5x10^{-6}$	1.169	1.090	1.058	1.006
$7x10^{-6}$	1.245	1.138	1.103	1.014
$9x10^{-6}$	1.310	1.128	1.129	1.018
$11x10^{-6}$	1.463	1.182	1.224	1.033

3.5. Electrochemical technique:

Electrochemical techniques are based on current and potential measurements. According to the choice of the technique accurate and confidential data, concerning the corrosion process can be obtained.

3.5.1- Galvanostatic polarization technique:

Galvanostatic polarization curves of α-brass in 2 mol l^{-1} nitric acid in the absence and presence of different concentrations of compound (**a**) at 30°C are illustrated in Figure (9). Similar galvanostatic polarization are obtained in the presence of different concentrations of the other compounds (**b, c, d**), but not shown. The numerical values of the variation of corrosion current density ($i_{corr.}$), corrosion potential ($E_{corr.}$), Tafel slopes. (β_a and β_c), percentage inhibition efficiency (%In.) and degree of surface coverage (θ) with the concentrations of compound (**a**) are given in Table (7). From this Table and Figures (9) and similar ones can conclude that:

1- The cathodic and anodic curves obtained exhibit Tafel-type behavior. Addition of arylazo indole compounds increases both cathodic and anodic overvoltages and causes mainly parallel displacement to more negative and positive values, respectively.

2- The corrosion current density ($i_{corr.}$) decreases with increasing the concentration of arylazo indole compounds, which indicates that the presence of these compounds retards the dissolution of α-brass in 2 mol l^{-1} nitric acid solution and the degree of inhibition depends on the concentration and type of the inhibitor present.

3- The order of decreased inhibition efficiency of arylazo indole compounds is: **a > b > c > d**. This is also in agreement with the observed order of percentage inhibition efficiency calculated from weight loss method.

4- The data suggested that these compounds act as mixed-type inhibitors *i.e.* retards both the anodic and cathodic reactions but the cathode is more polarized when an external current was applied.

5- The corrosion potential ($E_{corr.}$) values shifted to more negative values by increasing the concentration of arylazo indole compounds.

Figure (10) shows the relation between (θ) and log C. The obtained plots have S-shape indicating that the adsorption of organic compounds (**a-d**) obeys Frumkin's adsorption isotherm.

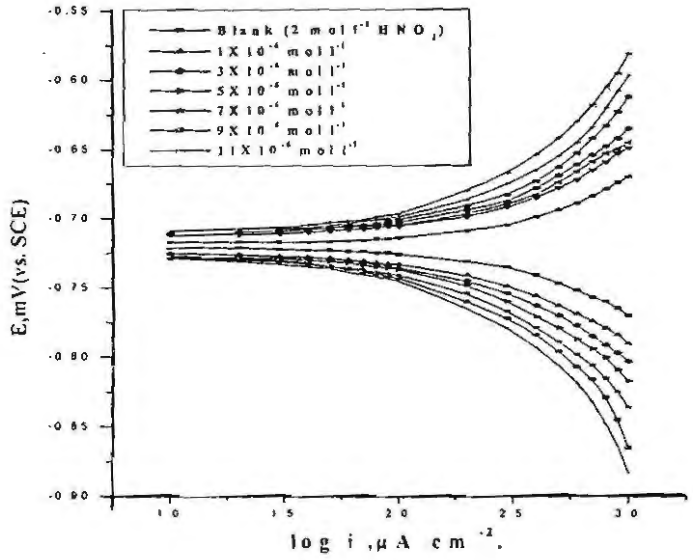

Fig.(9): Galvanostatic polarization curves of α-brass in 2 mol l^{-1} HNO_3 alone and containing different concentrations of compound (a) at 30°C.

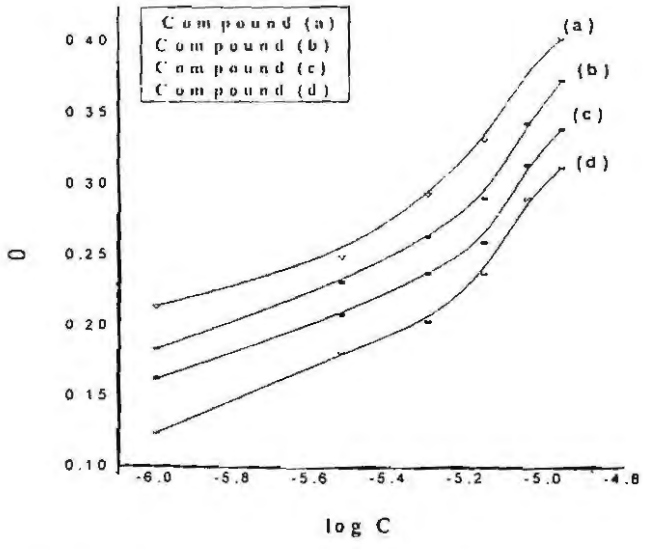

Fig. (10): Log(C) vs. θ curves for the different compounds.

Table (6): Percent inhibition efficiency from galvanosatic polarization of α-brass containing various concentrations of all compounds used in 2 mol l^{-1} HNO_3 at 30°C.

Concentration (M)	Inhibition efficiency (%In)			
	a	b	c	d
$1x10^{-6}$	21.38	18.4	16.3	12.4
$3x10^{-6}$	24.9	23.1	20.8	18.1
$5x10^{-6}$	29.35	26.3	23.7	20.3
$7x10^{-6}$	33.12	28.98	25.9	23.7
$9x10^{-6}$	37.98	34.2	31.32	28.9
$11x10^{-6}$	40.18	37.2	33.8	31.1

Table (7): The effect of concentration of compound (a) on the free corrosion potential ($E_{corr.}$), corrosion current density ($i_{corr.}$), Tafel slopes (β_a & β_c), %In and degree of surface coverage (θ) for α-brass in 2 mol l^{-1} HNO_3 at 30°C.

Concentration, M.	$-E_{corr.}$, mV	$i_{corr.}$, μA cm	β_a, mV dec	$-\beta_c$, mV dec	θ	%In
0.0	720	168.63	55	57	-	-
$1x10^{-6}$	724	123.58	80	68	0.214	21.4
$3x10^{-6}$	724	126.64	86	77	0.249	24.9
$5x10^{-6}$	725	119.14	90	87	0.293	29.3
$7x10^{-6}$	726	112.78	97	97	0.331	33.1
$9x10^{-6}$	726	104.59	105	100	0.380	38.0
$11x10^{-6}$	727	100.87	122	110	0.402	40.2

3.5.2. Chemical structure and corrosion inhibition of α-brass:

Inhibition of the corrosion of α-brass in 2 mol l^{-1} HNO_3 solution by some arylazo indole derivatives is determined by galvanostatic polarization measurements and was found to depend on concentration, nature of metal, the mode of adsorption of the inhibitors and surface conditions. Skeletal representation of the proposed mode of adsorption of the investigated arylazo indole derivatives as shown in Figure (11) and clearly indicates the active adsorption centers in the arylazo indole derivatives. These compounds can be adsorbed through the N-atom of the

pyridine ring. It was concluded that the mode of adsorption depends on the affinity of the metal towards the π-electron clouds of the ring system **[Samkarapaapaavinasam & Ahmed (1992)].** Metals such as Cu and Fe, which have a greater affinity towards aromatic moieties, were found to adsorb benzene rings in a flat orientation. Thus, it is reasonable to assume that the tested inhibitors are adsorbed in a flat orientation through the N- atom of the pyridine ring and O- atom of the OCH_3 group. The order of decreasing the percentage inhibition efficiency of the investigated inhibitors in the corrosive solutions was as follow: **a > b > c > d**. This behavior can be rationalized on the basis of the structure-corrosion inhibition relationship of organic compounds. Linear Free Energy Relationships (LFER) has previously been used to correlate the inhibition efficiency of organic compounds with their Hammett constituent constants (σ) **[Madkour et al., (1995)].** The LFER or Hammett relation is given by **[Donahu & Nobe (1965); Vasseghi & Nobe (1979) and Szklavska et al., (1973)].**

$$\text{Log R (rate of corrosion)} = -\rho\sigma \qquad (7)$$

Where ρ is the reaction constant, those constituents which attract electrons from the reaction center are assigned positive σ values and those which are electron donating have negative σ values. Thus, σ is a relative measure of the electron density at the reaction center. The slope of the plot of log (rate) vs. σ is ρ, and its sign indicates whether the process is inhibited by an increase or decrease of the electron density at the reaction center. The magnitude of ρ indicates the relative sensitivity of the inhibition process to electronic effects. Figure (12) shows that indole derivatives **(a-d)** give a good correlation. The large positive slope of the correlation line (ρ= +0.994) shows a strong dependence of the adsorption character of the reaction center on the electron density of the ring. The strong dependence of the adsorption character of the reaction center on the electron density of the ring may be due to the fact that in this type of derivatives the center of adsorption is conjugated to the ring. Compound **(a)** has the highest percentage inhibition efficiency, this due to the presence of *p*-OCH_3 group which is an electron repelling group with negative Hammett constant (σ= -0.27) this group will increase the electron charge density on the molecule. Compound **(b)** comes after compound **(a)**, this is due to the presence of *p*-CH_3 group which is an electron donating group with negative Hammett constant (σ= -0.17), Also this group will increase the electron charge density on the molecule but with lesser amount than *p*-OCH_3 group in compound **(a)**. Compound **(c)**

with Hammett constant (σ= 0.0) comes after compound (**b**) in percentage inhibition efficiency, because H- atom in *p*-position has no effect on the charge density on the molecules. Compound (**d**) comes after compound (**c**) in percentage inhibition efficiencies. This is due to *p*-NO_2 groups is electron withdrawing group with positive Hammett constants (σ= +0.78) and its order of inhibition depends on the magnitude of its withdrawing character.

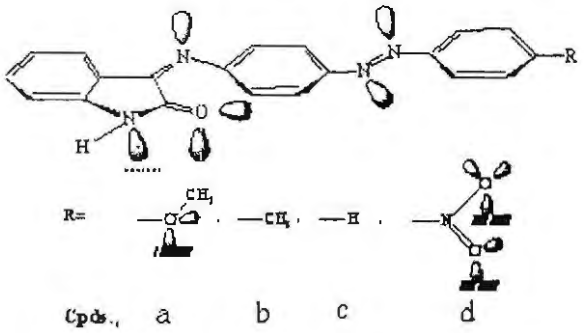

Fig. (11): Skeletal representation of the mode of adsorption of indole compounds.

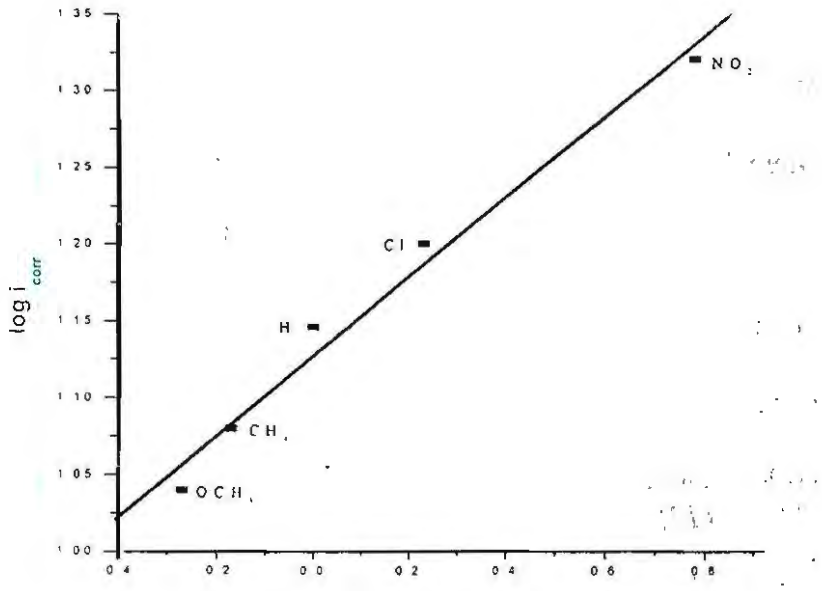

σ_p (Substituent constant)

Fig.(12): Relation between log corrosion current density, log i_{corr}, and Hammett constants. σ_p of the substituent from polarization measurements.

REFERENCES

Ammar I. A., Darwish S., and Etman M., *Electrochim. Acta.* (1968), *13,* 485.

Aramaki K. and Hackerman N., *J.Electrochem.Soc.* (1969), *116,* 568.

Cahskan N.; Bilgic S., *Appl. Surf. Sci.,* (2000), *153, 128.*

Chatterjee P.; Banerjee, M. K. and Mukherjee P., *Ind. J. Technol.,* 1991, *29 (5),* 191.

Donahu F. M., and Nobe K., *J. Electrochem. Soc.,* (1965), *112,* 886.

Hackerman, N.; Snavely, E. S. Jr. and Payne, J. S. Jr., *J.Electrochem.Soc.* (1966), *113(7),* 677.

Hang J., Yao L., Ruang E., and Zou J., *J.Chim.Soc.Corros.Prot.* (1988), *8,* 189.

Haquea M. M. and Faris Ismailb A., *Advanced Materials Research,* (2008), *33-37,* 7-12.

Jestonek M. and Szklarska Z. Smialowska, *Corros. Sci.* (1983), *23,* 183.

Madkour L. H., Elmorsi M. A., and Ghoneim M. M., *Monatsh. Chem.* (1995), *126 (10),* 1087.

Mihit M., El Issami S., Bouklah M., Bazzi L., Hammouti B., Ait Addi E., Salghi R. and Kertit S., *Applied Surface Science,* (2006), *252 (6),* 2389-2395.

Murakawa T.; Kato T.; Naguara S. and Hackerman N., *Corros. Sci.,* (1968), *8(7),* 483.

Otieno-Alego V., Hope G. A., Flitt H. J., Cash G. A., and Schweinsberg D. P., *Corros. Sci.,* (1992), *33,* 1719.

Rawat N. S. and Udayabhanu G., *Proceedings of 10th International Congress on Metallic Corrosion organized by CECRI in Madras, India,* (1987), *Vol.III,* 2963.

Rehan H. H., Al-Moubarak N. A., Al-Rafai H. A., *Portugaliae Electrochimica Acta,* (2003), *21(2).*

Samkarapapaavinasam S. and Ahmed M. F., *J.Appl Electrochem.,* (1992) *22*, 390.

Stevanovic J., Skibina L. J., Stefanovic M., Despic A., Jovic V. D., *J. Appl. Electrochem.* (1992), *22*, 172.

Szklavska Z. Smialowska and Kaminski M., *Corros. Sci.,* (1973), *13.*

Vasseghi S. and Nobe K.,*Corrosion,* (1979), *35*, 300.

تشييد صبغات جديدة ودراسة تأثيرها على تآكل بعض سبائك التقنية

عبدالعزيز السيد فوده – هـدى محفـوظ

قسم الكيمياء – كليه العلوم – جامعه المنصوره – المنصورة – مصر

التركيز (logC) لهذه المركبات (a-d) امتزاز فيزيائي يتم من خلال المراكز الغنية بالالكترونات فى هذه يهدف هذا البحث الى دراسة تاثير المشتقات المختلفة لمركبات الاريـل ازو اندول على معدل عملية التاكل نظرية التآكل و أسبابه وأشكاله و طرق معاجته بالاضافة الى أستعراض الابحاث المنشورة على تآكل الالفابراس فى محلول ٠,٢ مولارى من حمـض النيتريك. يرمى هذا البحث الى دراسة المركبات (a-d) كمثبطات للتآكل ولقـد تمـت هـذه الدراسة بطريقتين:

الاولى: هى الطريقة الكيميائية (فقد الوزن):

توضح هذه الطريقة ان مقدار كفاءة التثبيط للاضافات المختلفة تزداد بزيادة تركيـز تلك الاضافات فى وسط التآكل، حيث ان مساحة السطح المغطى بتلك الاضافات يقلـل مـن تآكل الالفابراس. ولقد اوضحت هذة الطريقة أن ترتيب هذة المركبات من حيث كفاءة التثبيط كالتالى:. **a > b > c > d** ولقد اظهرت العلاقة بين درجة تغطية الـسطح (θ) ولوغـاريتم المركبات، وأن عملية الامتزاز تتبع أيزوثرم فرومكن. ولقد تم أيضا دراسـة تـأثير درجـة الحرارة على كفاءة التثبيط فى نطاق حرارى من ٣٠°م إلى ٥٠°م، ولقد لوحظ ان معدل تآكل الالفابراس يزداد بزيادة درجة الحرارة مما يدل على انه امتزاز فيزيائى لتلك المشتقات على سطح المعدن.

الثانية هى طريقة الاستقطاب الجالفانوستاتيكى:

ولقد كشفت هذه الطريقه عن ان كثافة تيار التآكل تقل بزيادة تركيز مركبات الاريل ازو اندول والذى يوضح ان وجود تلك المركبات يقلل تآكل الالفابراس من ثم تم ترتيب هـذه المركبات طبقا لزيادة كفاءة التثبيط كالاتى: **a > b > c > d** ومن خلال العلاقة بين درجـة تغطية السطح(θ) ولوغاريتم التركيز (log C) لهذه المركبات(a-d) تبين ان عملية الامتزاز تتبع أيزوثرم فرومكن والتى تتوافق مع النتائج التى تم الحصول عليها من طريقة فقد الوزن.